

A linear array of 980 nm VCSEL and its high temperature operation characteristics*

Zhang Yan(张岩)^{1,2}, Ning Yongqiang(宁永强)^{1,†}, Wang Ye(王焱)^{1,2}, Liu Guangyu(刘光裕)^{1,2},
Wang Zhenfu(王贞福)^{1,2}, Zhang Xing(张星)^{1,2}, Shi Jingjing(史晶晶)^{1,2},
Zhang Lisen(张立森)^{1,2}, Wang Wei(王伟)^{1,2}, Qin Li(秦莉)¹,
Sun Yanfang(孙艳芳)¹, Liu Yun(刘云)¹,
and Wang Lijun(王立军)¹

(1 Key Laboratory of Excited State Processes, Changchun Institute of Optics, Fine Mechanics and Physics, Chinese Academy of Sciences, Changchun 130033, China)

(2 Graduate University of the Chinese Academy of Sciences, Beijing 100049, China)

Abstract: A 980 nm bottom-emitting vertical-cavity surface-emitting laser linear array with high power density and a good beam property of Gaussian far-field distribution is reported. This array is composed of five linearly arranged elements with a 200 μm diameter one at the center, the other two 150 μm and 100 μm diameter ones at both sides of the center with center to center spacing of 300 μm and 250 μm , respectively. A power of 880 mW at a current of 4 A and a corresponding power density of up to 1 kW/cm^2 is obtained. The temperature dependent characteristics of the linear array are investigated. The thermal interaction between the individual elements of the VCSEL linear array is smaller due to its optimized element size and device spacing, which make it more suitable for high power applications. A peak power of over 20 W has been achieved in pulsed operation with a 60 ns pulse length and a repetition frequency of 1 kHz.

Key words: VCSEL; array; temperature characteristics; high power

DOI: 10.1088/1674-4926/30/11/114008

PACC: 4255P; 4260B

EEACC: 4320J

1. Introduction

Vertical-cavity surface-emitting lasers (VCSEL) have become the most promising semiconductor laser source due to their most remarkable features such as the circular output beam, monolithic two-dimensional array processing, on-wafer testing, and single longitudinal mode^[1,2]. VCSEL with output powers of a few mW have been widely used in optical communications, scanning, massive parallel optical interconnections, and so on^[3-5]. Applications in solid-state laser pumping, numerous medical applications, high-resolution printing and free-space optical communication are revealing a growing market for high-power diode lasers^[6-8]. In particular, high-power laser devices with a good quality laser beam and narrow spectral width in the 940–980 nm wavelength range are desired for the pumping of Er- or Yr-doped fiber amplifiers or fiber lasers^[9,10]. To increase the overall optical output power, the total lasing area of VCSEL has to be enlarged by increasing the active area of single devices or integrating densely packed arrays^[11,12]. The temperature dependence of VCSEL has been an important issue in their development, due to the lower efficiency caused by higher thermal resistance and severe conversion from electric power to heat. Lower conversion efficiency from electric power to optical power will hamper the device's ability to generate high power, especially in VCSEL arrays.

Conventional VCSEL arrays are usually two-dimensional uniform arrays with elements of the same diameter and spacing. The dimension of individual elements is designed to be quite small to reduce the threshold current of the VCSEL array. This configuration is accompanied by an increase in the thermal resistance because the thermal resistance of the element is inversely proportional to the active diameter^[13]. In addition, the thermal crosstalk between the individual elements not only results in severe problems in heat dissipation but also limits the overall output characteristics of the arrays. The higher the density of the array, the worse the crosstalk thermal effect is. Furthermore, the circular profile of light beams emitted from the elements in a conventional array will superimpose and form a periodic intensity distribution with a series of peaks at far field, which causes the beam quality of VCSEL array to deteriorate and reduces the fiber-optic coupling efficiency. In this paper, we report a 980 nm bottom-emitting VCSEL linear array with a new arrangement unlike the conventional structure. This linear array is composed of five symmetrically-arranged elements of 200 μm , 150 μm and 100 μm diameter, with center spacings of 300 μm and 250 μm , respectively. By using the optimized arrangement, a good beam property of Gaussian far-field distribution is demonstrated and an output power of 880 mW with a high power density of 1 kW/cm^2 is obtained. The temperature dependent characteristics of linear arrays are

* Project supported by the National Natural Science Foundation of China (Nos. 60636020, 60676034, 60706007, 60577003, 60876036).

† Corresponding author. Email: ningyq@ciomp.ac.cn

Received 19 May, revised manuscript received 8 July 2009

© 2009 Chinese Institute of Electronics

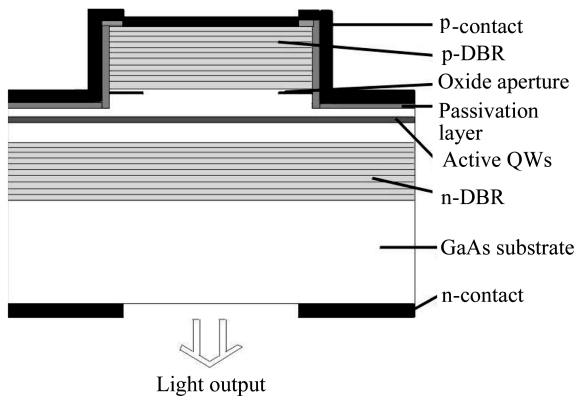


Fig. 1. Schematic diagram of VCSEL structure.

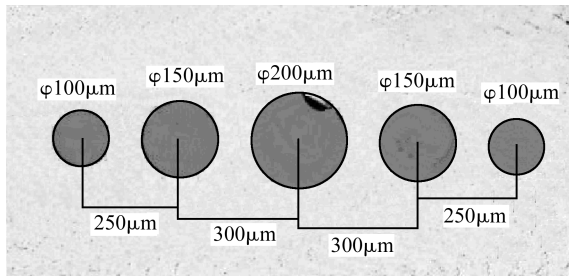


Fig. 2. Picture of VCSEL linear array.

investigated. It is concluded that the linear array is more suitable for high temperature operation due to its improved arrangement. The linear array characteristics under short-pulsed operation are also obtained.

2. Device structure and processing

A schematic cross-section view of a VCSEL structure is displayed in Fig. 1. VCSEL structures with 28.5 pairs of silicon-doped n-type distributed Bragg reflectors (DBR), InGaAs/GaAs quantum wells, and 30 pairs of carbon-doped p-type DBRs are grown by metal-organic chemical vapor deposition (MOCVD) on (001)-oriented n-GaAs substrate. Both DBRs consist of alternating $Al_{0.9}Ga_{0.1}As$ and $Al_{0.1}Ga_{0.9}As$ quarter-wavelength layers with graded interfaces to reduce series resistance. The active region is composed of three 8 nm thick $In_{0.2}Ga_{0.8}As$ quantum wells (QWs), which are embedded in 10 nm thick GaAs barriers and surrounded by AlGaAs cladding. A single 30 nm thick $Al_{0.98}Ga_{0.02}As$ layer is inserted above the p-type cladding layer in a node of the calculated standing wave pattern for selective oxidation.

A device picture of the linear array is shown in Fig. 2. This array is composed of five linearly arranged elements with the maximum diameter one of 200 μm at the center, 150 μm and 100 μm diameter ones at both sides of the center with center to center spacings of 300 μm and 250 μm , respectively. The purpose of this arrangement is to obtain a tradeoff between threshold current, output power and thermal resistance.

Wet chemical etching was used to define a circular mesa and to expose the layer of $Al_{0.98}Ga_{0.02}As$ for oxidation. The oxidation was carried out in a water vapor atmosphere using nitrogen as the carrier gas at 420 $^{\circ}C$ to form the current apertures. A SiO_2 passivating layer was deposited on the surface to

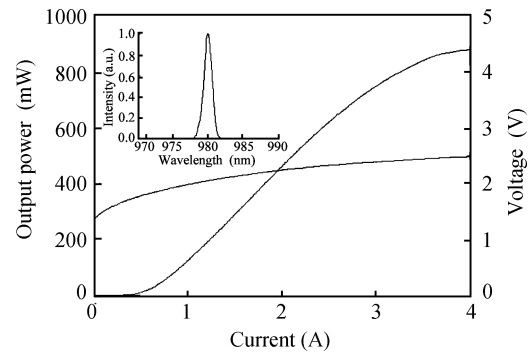


Fig. 3. $L-I-V$ characteristics of the VCSEL linear array. Inset: Measured lasing spectrum at injection current of 4 A.

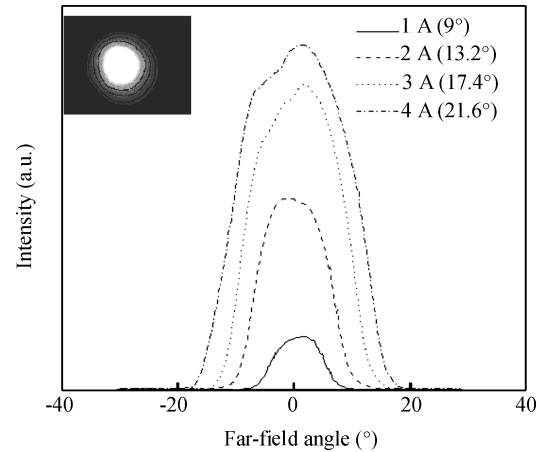


Fig. 4. Far-field angles of the linear array.

avoid short circuits when soldering the device on the heatsink. After selective etching of the SiO_2 film to form the p-side contact window, TiPtAu was evaporated on the mesa using electron beam deposition. The substrate was thinned and polished down to a thickness of 170 μm in order to reduce absorption losses. At the bottom of the GaAs substrate, the light emission window was surrounded by an n-type AuGeNi/Au electrode. Finally, the device was p-side down soldered upon a copper heatsink with indium solder to ensure efficient heat dissipation.

3. Device performance

The light-current-voltage ($L-I-V$) characteristic is shown in Fig. 3. The threshold current (I_{th}) of the device is about 0.61 A with a corresponding threshold current density of 739 A/cm^2 , and the differential resistance (R_d) is 0.13 Ω . The maximum CW optical output power is up to 0.88 W at a current of 4 A at room temperature. The corresponding optical power density averaged over the total lasing area is 1 kW/cm^2 . The lasing wavelength at an injection current of 4 A is shown in the inset of Fig. 3, and the lasing peak wavelength is 979.9 nm, with FWHM of 1 nm.

The far field distributions of the linear array at different currents are shown in Fig. 4, and those of the conventional 4×4 two dimensional (2D) array with 80 μm element aperture size and 130 μm center spacing (maximum power is 0.35 W at 3 A) are shown in Fig. 5. For the 2D array, the individual

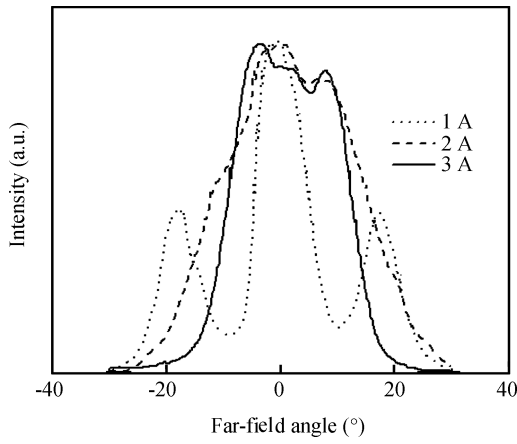
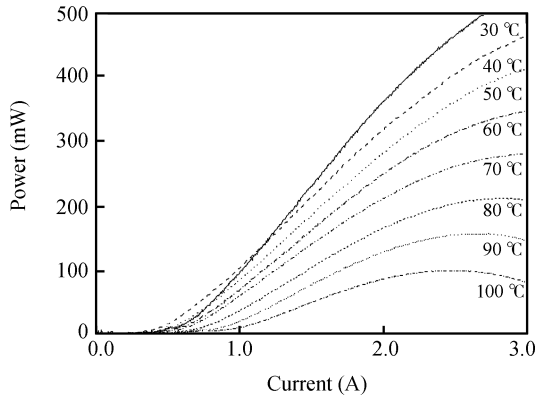


Fig. 5. Far-field angles of the 2D array.

Fig. 6. $L-I$ for a linear array at various temperatures.

element superimposes and forms a periodic intensity distribution with a series of peak values at far field. In contrast, the linear array with optimized center spacing, arrangement and intensity superposition of beams from all elements created an intensity maximum on the symmetry axis. For all driving currents the beam shape can be described by a Gaussian profile and the far field divergence angle at half-maximum intensity increases from 9° to 21.6° in an operating current range of 0 to 4 A. The inset is the far field picture captured by a CCD image-forming system at a current of 4 A. Due to the circularly symmetric patterns with low beam divergence angle, the beam of the linear array can be easily focused or collimated into a fiber in a simple butt-coupling arrangement for broad applications.

To investigate the temperature dependent characteristic of the VCSEL linear array, we measured the optical output power, the threshold current and the lasing wavelength at various heatsink temperatures. The $L-I$ characteristics of the linear array at heatsink temperatures varying from 30 to 100 °C which are precisely controlled by a thermoelectric couple are shown in Fig. 6. A drastic reduction of output power and slope efficiency occurs with increasing temperature, and the rollover of output power is more serious when the heatsink temperatures rise. The reason for this can be ascribed to the following. Under CW operation, the thermal resistance of the array's element produces excessive thermal due to power dissipation, thus increasing the self-heating, causing the junction temperature to rise and gain to decrease, and further raising the power

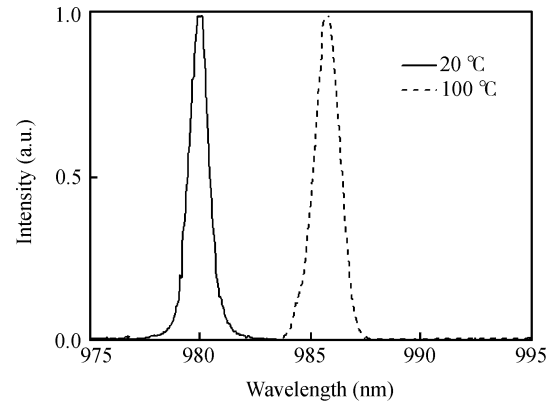


Fig. 7. Spectra of the linear array at 20 and 100 °C.

dissipation, which in turn further exacerbates the heating, and the cycle continues with the output power decreased until the junction temperature becomes too high for lasing. Furthermore, the thermal crosstalk effect between the array elements makes efficient heat diffusion of the array difficult.

In order to achieve high-performance for the VCSEL linear array with excellent operating characteristics over a broad range of temperatures, the cavity mode is designed misaligned on the red (long wavelength) side of the gain peak, and since the gain peak shifts at a much faster rate than the cavity mode with changing temperature, it will catch up to the cavity mode and become aligned with it at a higher temperature, at which the minimum threshold occurs. When the temperature becomes higher, the cavity mode is located on the blue side of the gain peak, and again causes de-tuning of gain-cavity mode, which causes I_{th} to increase. The lowest I_{th} of the linear array is observed when the heatsink temperature is 40 °C which is consistent with the design.

Figure 7 shows the lasing spectra of linear array under CW operation at temperatures of 20 and 100 °C. The lasing peak wavelength moves to 985.7 nm when the temperature rises to 100 °C. The wavelength shift of the linear array with temperature is about $0.07 \text{ nm}/^\circ\text{C}$, which is given by the cavity mode shift rate. It is apparent that even at high temperatures the device emits nominally in a single mode, there is no evident distortion, and the FWHM of the spectrum is spread to 1.2 nm at 100 °C.

Since VCSEL are not subject to catastrophic optical damage (COD), the VCSEL's arrays do not fail when operated at short pulses at many times their roll-over CW current, making them useful for high power applications. We developed a nanosecond power source delivering a peak current of 80 A with a pulse width of 60 ns and 1 kHz repetition frequency to drive the linear array. Under the pulse operation, the internal temperature rise (ΔT) of the VCSEL's array is given by^[14]

$$\Delta T = (I^2 R_d + IV_k) R_{\text{therm}} (1 - \eta) D, \quad (1)$$

$$D = P_w \times \text{PRF}, \quad (2)$$

where I is the injection current, R_d and R_{therm} are the resistant and thermal resistant, respectively, η is the power conversion efficiency, D is the duty cycle, and P_w and PRF are the pulse

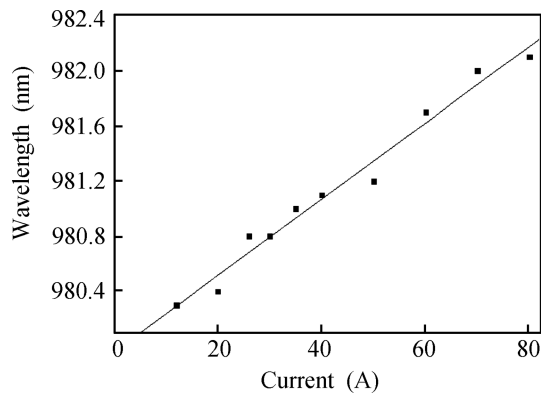
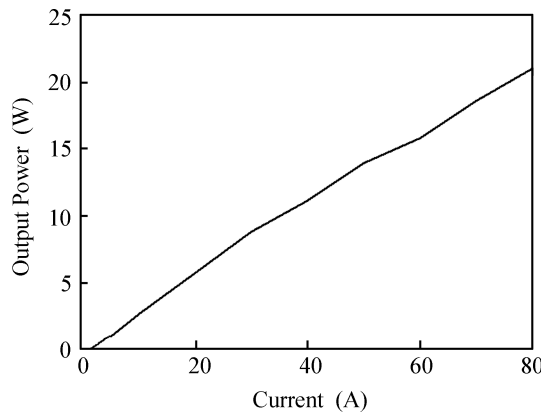


Fig. 8. Wavelength shift under pulse operation.

Fig. 9. P - I curve of the linear array under pulse current.

width and repetition frequency, respectively. The largest D of our nanosecond power source is 0.006%, so the ΔT can be ignored. This can be proved by the wavelength shift under nanosecond operation as indicated in Fig. 8. The lasing peak wavelength is shifted from 980.3 to 982.1 nm, a shift of only 1.8 nm, when the pulse operation changes from 12 to 80 A.

Figure 9 shows the output power characteristics of the linear array under short-pulse current operation. The VCSEL array emits about ten watts peak power without thermal rollover. With a 80 A pulse current (60 ns at 1 kHz), the output power of the linear array reaches 21 W. So the heat problem can be neglected and high output power can be expected when operated under short-pulse current.

4. Conclusion

In summary, we have reported a 980 nm bottom-emitting VCSEL linear array with high power density and a good beam property of Gaussian far-field distribution. This array is composed of 5 linearly arranged elements with a 200 μm diameter one at the center, 150 μm and 100 μm diameter ones at both sides of the center with center to center spacings of 300 μm and 250 μm , respectively. The threshold current is 0.61 A, and the differential resistance (R_d) is 0.13 Ω . The maximum output power is 880 mW, corresponding to 1 kW/cm² power density. The lasing peak wavelength is 979.9 nm, with a FWHM of 1 nm. Temperature dependent characteristics of the linear array are investigated. By setting the cavity mode misaligned on the

red (long wavelength) side of the gain peak, a VCSEL with excellent operating characteristics over a broad range of temperatures can be achieved. The threshold current of the linear array is minimized for a temperature of 40 °C. The thermal interaction between the individual elements of the VCSEL linear array is smaller due to its optimized arrangement, which make it more suitable for high power. When operated under short-pulse current, the heat problem can be neglected. A peak pulsed power of over 20 W has been achieved with the VCSEL linear array under a 60 ns pulse with 1 kHz repetition frequency pulsed operation.

References

- [1] Geels R S, Corzine S W, Coldren L A. InGaAs vertical-cavity surface-emitting lasers. *IEEE J Quantum Electron*, 1991, 27(6): 1359
- [2] Wiedenmann D, King R, Jung C, et al. Design and analysis of single-mode oxidized VCSEL's for high-speed optical interconnects. *IEEE J Sel Top Quantum Electron*, 1999, 5(3): 503
- [3] Jager R, Grabherr M, Jung C, et al. 57% wallplug efficiency oxide-confined 850 nm wavelength GaAs VCSEL's. *Electron Lett*, 1997, 33(4): 330
- [4] Ueki N, Nakayama H, Sakurai J, et al. Complete polarization control of 12×8-bit matrix-addressed oxide-confined vertical-cavity surface-emitting laser array. *Jpn J Appl Phys*, 2001, 40: 33
- [5] Amann M C, Ortsiefer M, Shau R, et al. Vertical-cavity surface-emitting laser diodes for telecommunication wavelengths. *Proc SPIE*, 2002, 4871: 123
- [6] Lan Y P, Chen Y F, Huang K F, et al. Oxide-confined vertical-cavity surface-emitting lasers pumped Nd: YVO₄ microchip lasers. *IEEE Photonics Technol Lett*, 2002, 14(3): 272
- [7] Gibson G M, Conroy R S, Kemp A J, et al. Microchip laser-pumped continuous-wave doubly resonant optical parametric oscillator. *Opt Lett*, 1998, 23: 517
- [8] Bouwmans G, Percival R M, Wadsworth W J, et al. High-power Er:Yb fiber laser with very high numerical aperture pump-cladding waveguide. *Appl Phys Lett*, 2003, 83: 817
- [9] Bjorlin E S, Kimura T, Chen Q, et al. High output power 1540 nm vertical cavity semiconductor optical amplifiers. *Electron Lett*, 2004, 40(2): 121
- [10] Wang D N, Lam K W. Tunable multiwavelength optical short pulse generation using cascaded fiber Bragg gratings and an erbium doped fiber amplifier in a simple self-seeding scheme. *Opt Commun*, 2004, 233: 191
- [11] D'Asaro L A, Seurin J F, Wynn J D. High-power, high-efficiency VCSELs pursue the goal. *Photonics Spectra*, 2005: 64
- [12] Seurin J F, Ghosh C L, Khalfin V, et al. High-power high-efficiency 2D VCSEL arrays. *Proc SPIE*, 2008, 6908: 1
- [13] Grabherr M, Miller M, Jäger R, et al. High-power VCSEL's: single devices and densely packed 2-D-arrays. *IEEE J Sel Top Quantum Electron*, 1999, 5(3): 495
- [14] Arai S, Suematsu Y, Itaya Y. 1.11–1.67 μm (100) GaInAsP/InP injection lasers prepared by liquid phase epitaxy. *IEEE J Quantum Electron*, 1980, 16(2): 197